ARTICLE NO. 79-1877R

C80-056

Flow Patterns and Aerodynamic Characteristics of a Wing-Strake Configuration

00001
00006

M.J. Liu,* Z.Y. Lü,† C.H. Qiu,† W.H. Su,† X.K. Gao,† X.Y. Deng,† and S.W. Xiong†
Beijing Institute of Aeronautics and Astronautics, Beijing, China

Surface oil flow visualizations, force tests, and pressure measurements were conducted at low, transonic, and supersonic speeds. Four flow patterns on a wing with strake at low speed have been found. The flow on the wing upper surface is affected and controlled by the formation, development, and breakdown of the strake vortices. The differences in flow patterns are reflected in the force and moment results. The lift increment results from the effect of the strake vortex not only on the inner panel but also on the outer panel. The nonlinear variations of the pitching moment are discussed. The lift increment is decreased with an increase in Mach number at transonic speeds, primarily because the flow over the wing without strake changes from leading edge separation to leading edge attached flow with shock-induced separation. An increase in the lift-drag ratio is due to the lift increase at low speeds and the drag decrease at supersonic speeds.

Nomenclature

C_L = lift coefficient, lift/qs
C_m = pitching moment coefficient about 0.15 c, moment/qsc
C_N = normal force coefficient
c = mean aerodynamic chord of wing without strake
ΔC_N = normal force coefficient increments, $C_{N_{\text{strake}}} - C_{N_{\text{basic}}}$
C_P = pressure coefficient
L/D = lift/drag ratio
M = Mach number
q = freestream dynamic pressure
S = area of wing without strake
α = angle of attack, deg
α_m = nominal angle of attack, deg
Λ = angle of leading edge sweepback of strake, deg

Introduction

In designing a modern supersonic combat airplane, it is most important to increase its maneuverability at high angles of attack at transonic speeds without deterioration of its required supersonic performance. The achievement of this objective would generally be handicapped, however, by the occurrence of flow separation. In order to improve the flow characteristics, a concept such as the wing with strake can be applied which utilizes flow separation instead of avoiding it. For the wing with strake the flow is separated from the strake leading edge and rolled up into a strong vortex, resulting in vortex-induced lift.

Flow observations and force tests have been carried out and discussed by previous investigators.[1-8] In the present investigation, surface oil flow visualizations, force tests, and wing surface pressure distribution measurements were conducted at low, transonic, and supersonic speeds from 1975 to 1977.[9-12] This paper is a general survey of the experimental studies made by the authors.

Experimental Investigation

Model and Apparatus

Low speed tests were conducted in a 1.5 m diam low speed wind tunnel at angles of attack up to 28 deg. The models are illustrated in Fig. 1. The wing without strake, i.e., basic wing, had leading edge sweepback of 30 deg. The 12 strakes had leading edge sweepback of 70-80 deg and area of 7-25% of the wing without strake. Models with different horizontal tail positions, twin vertical tails, and leading edge flaps were tested.

Tests were also conducted at transonic speeds for angles of attack up to 25 deg and at supersonic speeds for angles of attack up to 8 deg in a 0.6×0.6 m wind tunnel. The models of the wing-body configurations are illustrated in Fig. 2. The strakes had the same area of 17.6% of the wing without strake and three different leading edge sweepback angles.

The models were coated with black lacquer. A mixture of silicon oil, titanium dioxide, and kerosene was used for the surface oil flow visualizations.

Discussion of Results

Low Speed Flow Patterns

Surface oil flow visualizations of wing-body configurations having a wing with and without strake were carried out in the low speed wing tunnel. On increasing the angle of attack, four different types of flow on the upper surface of the wing with strake have been found. These are: 1) completely attached flow, 2) coexistence of strake vortex and attached flow, 3) coexistence of strake vortex and bubble votex, and 4) strake vortex breakdown. Of course, the angles of attack corresponding to these flow types are configuration dependent.

Completely Attached Flow

Completely attached flow occurs at very low angles of attack (about 0-2 deg). The oil flow lines on the wing upper surface are nearly streamwise.

Presented as Paper 79-1877 at the AIAA Aircraft Systems and Technology Meeting, Aug. 20-22, 1979; submitted Sept. 14, 1979; revision received Jan. 4, 1980.
Index categories: Aerodynamics; Configuration Design.
*Senior Research Engineer.
†Lecturer.

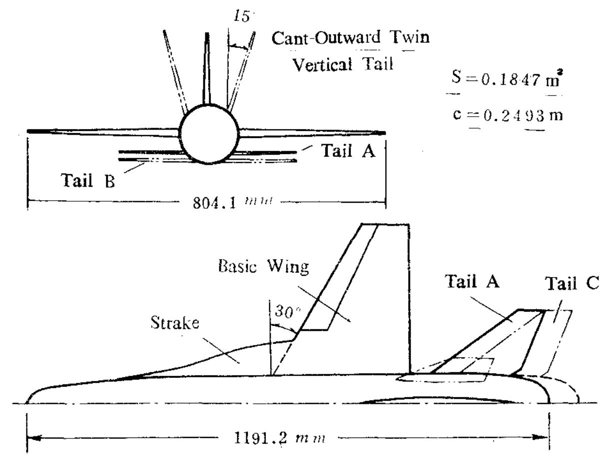

Fig. 1 Low speed models.

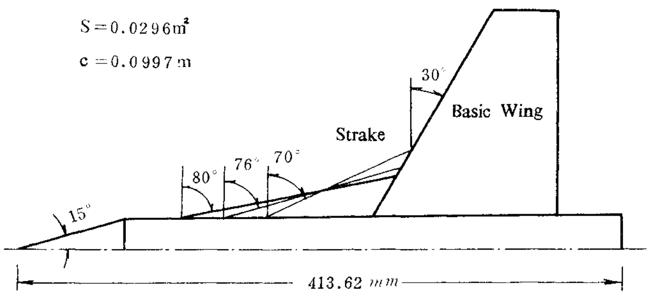

Fig. 2 High speed models.

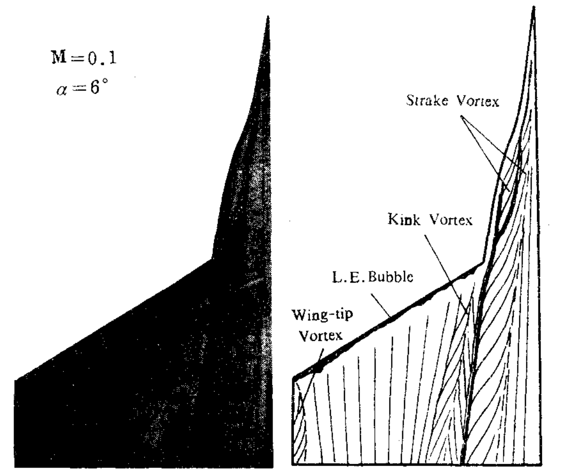

Fig. 3 Coexistence of strake vortex and attached flow, $\alpha = 6$ deg.

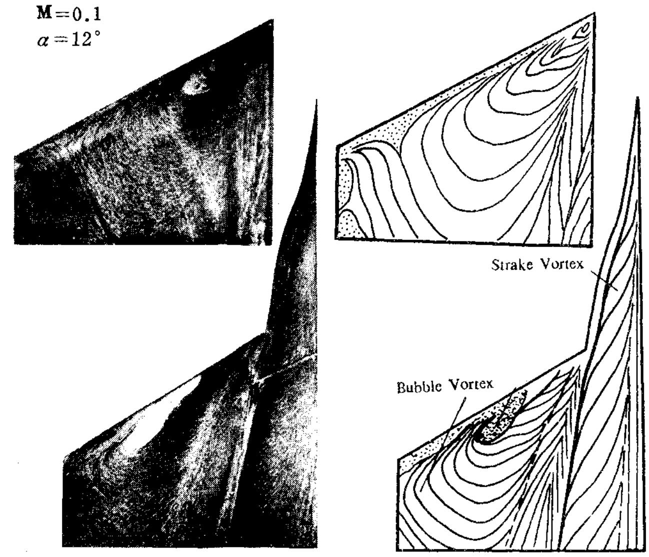

Fig. 4 Low speed flow pattern on wing with and without strake, $\alpha = 12$ deg.

Coexistence of Strake Vortex and Attached Flow

At low angles of attack (about 4-8 deg), the flow is separated from the strake sharp leading edge and rolled up into a spiral vortex over the wing. A typical oil flow pattern at an angle of attack of 6 deg is shown in Fig. 3. There are cross-flow, attached flow, and separated flow regions as well as reattachment and secondary separation lines on the upper surface at inboard wing stations. The flow is separated from the leading edge of the outer panel and then reattached on the surface, thus forming a leading edge bubble. The oil accumulation line is visible, but there is still a high degree of attached flow on the outer panel. The principal feature of the flow in this angle of attack range is, therefore, the coexistence of the strake vortex and attached flow. The cross-flow regions near the wing tip and the kink of the leading edge are induced by the wing tip vortex and kink vortex, respectively, the former being developed by flow separation from the side edge.

The strake vortex sheet separates the two mainstream flows moving in different flow directions from the upper and lower surfaces as in the case of a slender wing, but differs from the latter in that the vorticity of the wing with strake is fed from the strake leading edge up to the kink of the wing. The circumferential and axial velocities of the vortex core are high and the static and total pressures are low.

Coexistence of Strake Vortex and Bubble Vortex

At moderate angles of attack (about 8-16 deg) the strake vortex is more stable and strengthened. Moreover, a bubble vortex is formed and developed over the upper surface of the outer panel. Figure 4 shows a typical oil flow pattern on the wing with strake at $\alpha = 12$ deg. The flow pattern on the inner panel is nearly the same as that described above. However, on the outer panel there are reattached flow, cross-flow, and separated flow regions. The bubble vortex is developed from the bubble, it looks like the vortex from the surface oil flow observation and is different from the strake vortex as well as the bubble.

The flow pattern on the wing without strake at an angle of attack of 12 deg is shown in Fig. 4. Instead of a cross-flow region, there is a reversed flow as well as larger leading edge and wing tip separation regions. Comparing the flow patterns of the wings with and without strake, it is apparent that the strake vortex has a significant effect upon the outer panel flow. Upwash and outward sidewash are induced on it by the strake vortex. The sidewash velocity accelerates the flow on the outer panel and increases the kinetic energy of the boundary layer flow such that leading and side edge separations are diminished and the flow is greatly improved.

Strake Vortex Breakdown

At high angles of attack (higher than about 16 deg) the strake vortex breaks down. As the angle of attack is increased, the breakdown point moves forward. A typical flow pattern with strake vortex breakdown is shown in Fig. 5. The secondary separation line is deflected outward and defines the trumpet-like shape of the burst strake vortex. After the breakdown of the strake vortex, the vortex core radius grows larger, the circumferential and axial velocities are reduced, and the static and total pressures will be recovered.

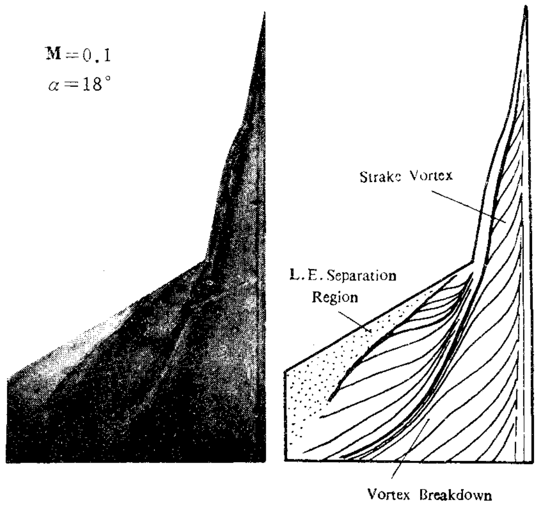

Fig. 5 Strake vortex breakdown, α = 18 deg.

Aerodynamic Characteristics at Low Speed

The variations of lift and pitching moment with angle of attack at low speed for wing-body configurations having a wing with and without strake are given in Figs. 6 and 7, respectively. The differences described above in the flow patterns at the different angles of attack are reflected in the force and moment results.

Completely Attached Flow

The lift and moment curves are linear at very low angles of attack, because there is no separation on the surface and the strake vortex is not formed yet. Adding the strake to the wing results in a forward movement of the aerodynamic center. For the configurations tested, the forward movement is about 8% of the mean aerodynamic chord. Adding the strake to the wing brings about a variation in chordwise pressure distribution on the inner panel, i.e., the leading edge suction peak moves forward. Adding the strake has little effect on the lift coefficient, however, because the increase in lift associated with the strake is offset by a detrimental interference effect of the strake on the aft inner panel.

Coexistence of Strake Vortex and Attached Flow

The lift slope is increased slightly and there is a nose-up moment at low angles of attack. This can be attributed to the formation of the strake vortex, the bubble having only a nominal effect. The nose-up moment comes primarily from the vortex-induced lift on the strake itself concurrent with less contribution of the aft portion of the inner panel. Vorticity is shed only up to the kink.

Coexistence of Strake Vortex and Bubble Vortex

The lift curves of the wing with and without the strake show that adding the strake results in a large increment in lift at moderate angles of attack. For the wing-body configurations tested, the lift increment is about 38% of the lift of the wing

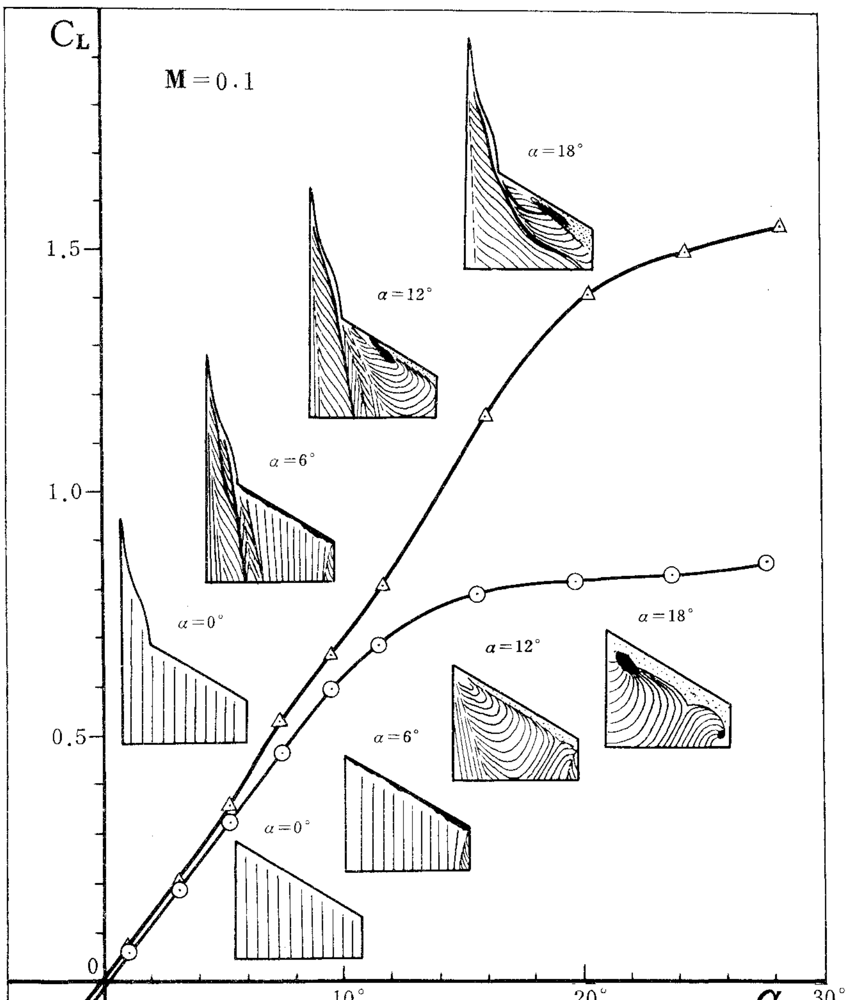

Fig. 6 Lift curves for wing with and without strake.

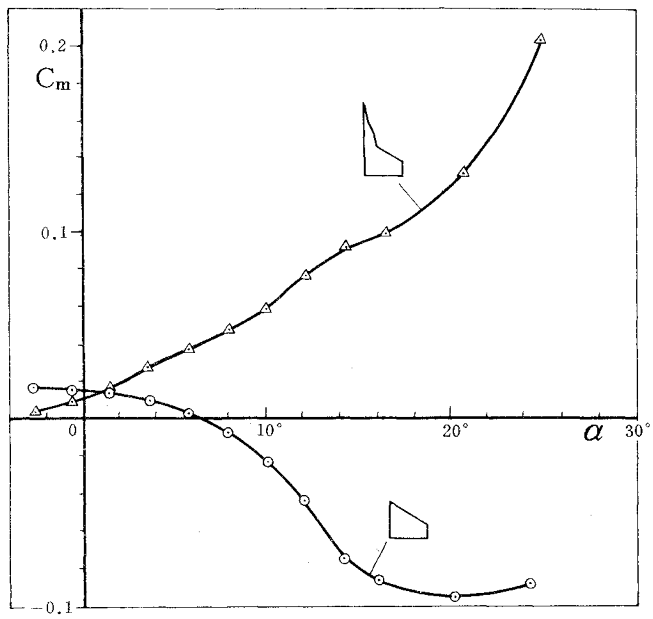

Fig. 7 Pitching moment curves for wing with and without strake.

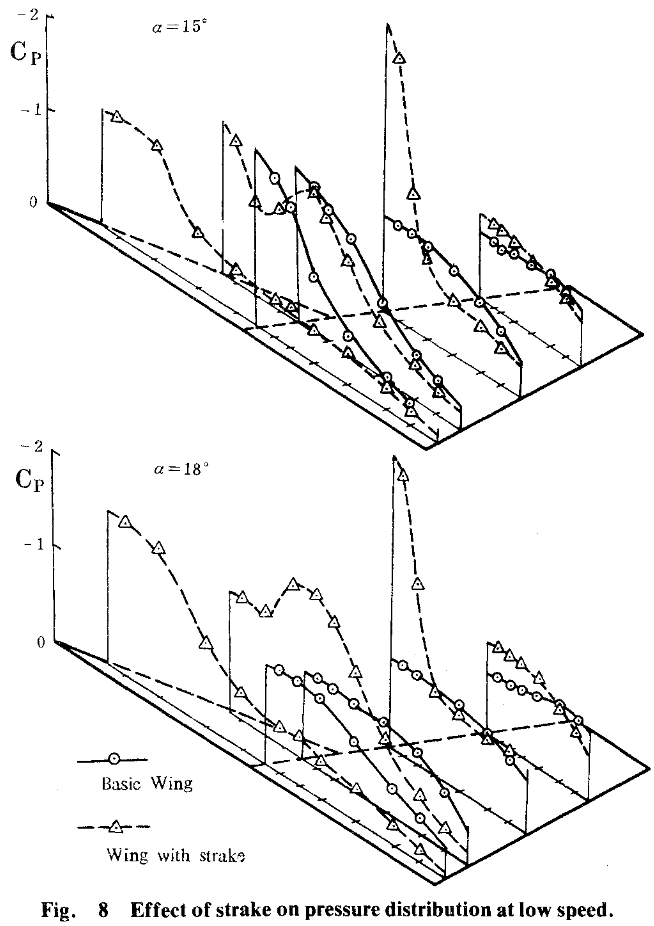

Fig. 8 Effect of strake on pressure distribution at low speed.

without strake at an angle of attack of 15 deg. The lift is increased due to the effects of the strake vortex and decreased by the bubble vortex. The strake vortex affects not only the strake itself and the aft inner panel, but also the outer panel. These effects are dependent upon the angle of attack.

The stable strake vortex has a great effect on the strake itself. The high circumferential and axial velocities of the strake vortex induce a low pressure on the strake, and a vortex lift is generated. The stable strake vortex has also a great

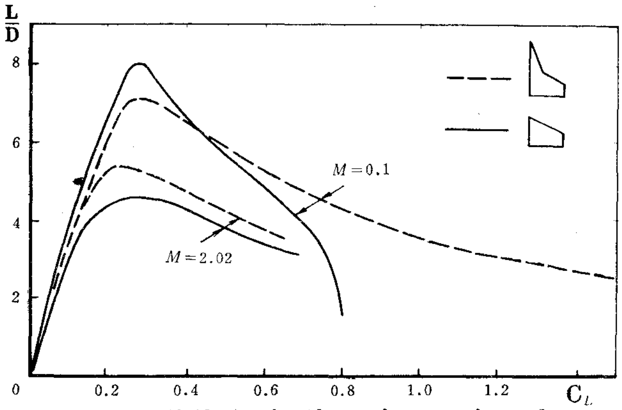

Fig. 9 Lift/drag ratio at low and supersonic speeds.

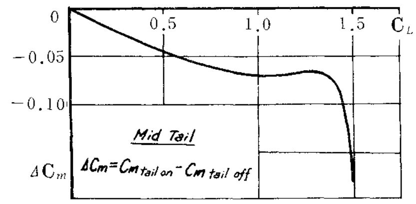

Fig. 10 Effect of lift on horizontal tail contribution to pitching moment (moment reference point, 0.25 c).

effect on the outer panel. The sidewash and upwash effects of the strake vortex will delay flow separation. As a result, the separation region is greatly diminished and the lift increment becomes larger. The pressure distributions show that about 43% of the lift increment comes from the outer panel at an angle of attack of 15 deg, as shown in Fig. 8.

Strake Vortex Breakdown

The lift curve slope decreases and a sudden nose-up moment appears at high angles of attack (higher than about 16 deg). These large changes are due to the breakdown of the strake vortex. For the wing-body configurations tested, the lift increment is about 60% of the lift of the wing without strake at an angle of attack of 18 deg. From the pressure measurements shown in Fig. 8, about 45% of this lift increment comes from the outer panel.

The variation of lift/drag ratio with angle of attack at low speed is given in Fig. 9. The lift/drag ratio of the wing with strake is larger than that of wing without strake only at high angles of attack. This increase in lift/drag ratio results mainly from the increase in lift.

Nonlinearity of Pitching Moment

One of the principal problems encountered in utilizing the wing with strake is the nonlinearity of the pitching moment. It occurs with the formation and breakdown of the strake vortex. For an airplane having a wing with strake, the nonlinear pitching moment comes not only from the wing but also from the horizontal tail.

Figure 10 presents the tail contribution to pitching moment, i.e., the moment coefficient difference of an airplane model with and without the horizontal tail for a range of lift coefficient. The nonlinearity arising from the tail is affected by the strake vortex, this effect depending upon the angle of attack. For example, at low to moderate lift coefficients, there is a nose-up moment from the horizontal tail. This is due to the downwash on the tail from the strake vortex. As the angle of attack is increased, the strake vortex is strengthened with subsequent increase in the downwash and the nonlinear pitching moment. At high lift coefficients, there is a nose-down moment associated with a forward progression of the strake vortex breakdown point ahead of the horizontal tail with subsequent reduction in the downwash on the tail.

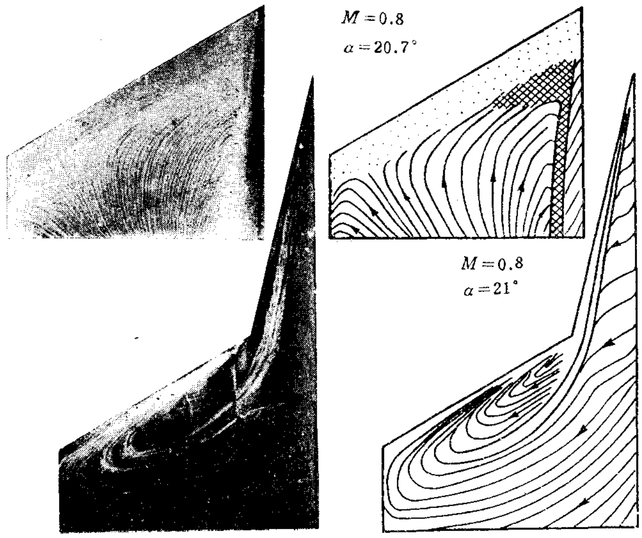

Fig. 11 Effect of strake on flow patterns, $M = 0.8$, $\alpha_m = 20$ deg.

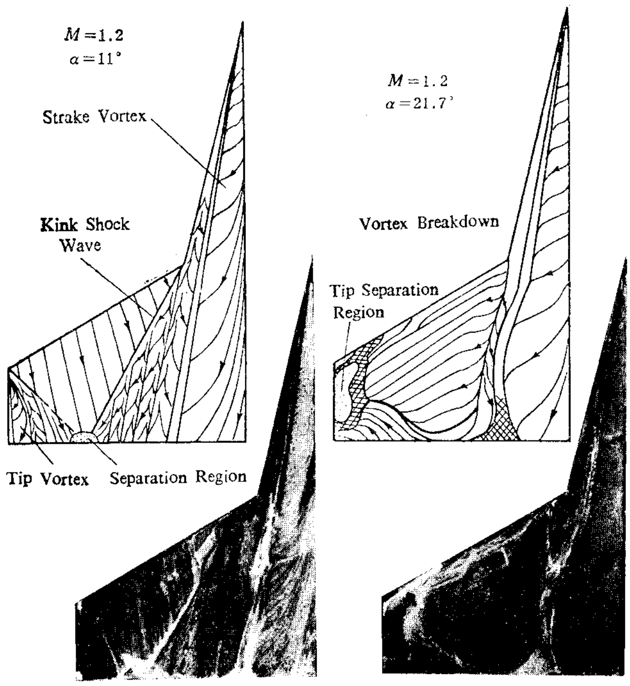

Fig. 12 Effect of angle of attack on flow patterns, $M = 1.2$.

In order to reduce the nonlinear pitching moment of the airplane having a wing with strake, the effects of wing planform and leading edge flap deflection in addition to horizontal and vertical tail arrangments have been investigated.

The downward deflection of the leading edge flap will reduce the nonlinearity of the pitching moment and delay the occurrence of the nose-up increments to a higher lift coefficient. Because of the reduction and aft movement of the leading edge suction peak, a decrease in the nonlinear pitching moment occurs at moderate angles of attack. Moving the tail downward and aft will reduce the nonlinearity of the pitching moment. The horizontal tail will be farther away from the strake vortex, thus alleviating the effect. The nonlinear pitching moment can also be reduced by means of a cant-outward twin vertical tail arrangement and anhedral of the horizontal tail and by sweeping the wing trailing edge forward.

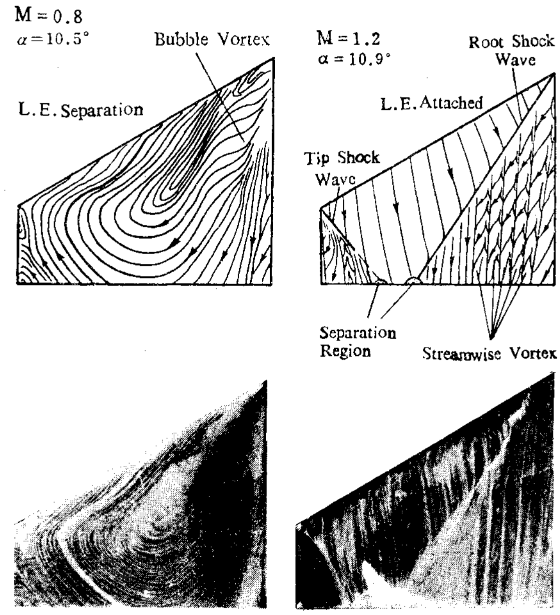

Fig. 13 Effect of Mach number on flow patterns, $\alpha_m = 10$ deg.

Transonic Flow

Flow Patterns

The oil flow patterns of the wing with and without strake at Mach 0.8 at a nominal angle of attack of 20 deg are shown in Fig. 11. For the wing with strake the strake vortex breaks down, a large cross-flow region and a small separation region being clearly visible. The wing without strake shows a completely reversed flow. It is obvious that the outer panel flow is greatly improved with the addition of the strake.

The oil flow patterns of the wing with strake at Mach 1.2 at nominal angles of attack of 10 and 20 deg are shown in Fig. 12. As the angle of attack is increased from 10 to 20 deg, the flow pattern changes from leading edge attached flow to leading edge separated flow. There is a coexistence of the strake vortex and leading edge attached flow with shock-induced separation at an angle of attack of 10 deg. The oil flow pattern shows a cross-flow region on the inner panel. On the outer panel there is a high degree of leading edge attached flow with visible streamwise vortices behind the kink shock. Coexistence of the strake vortex breakdown and leading edge separation is evident at an angle of attack of 20 deg. The oil flow pattern shows the cross-flow and a kink on the secondary separation line on the inner panel. On the outer panel, cross-flow, reversed flow, and side-edge separated flow regions are seen.

The oil flow patterns of the wing without strake at Mach 0.8 and 1.2 at a nominal angle of attack of 10 deg are presented in Fig. 13. This shows that as the Mach number increases from 0.8 to 1.2, the flow pattern is changed from leading edge separated flow to the leading edge attached flow with shock-induced separation. The leading edge pressure distribution passes from subsonic to supersonic type, and the chordwise adverse pressure gradient is decreased.

Aerodynamic Characteristics

The variations of normal force with angle of attack and pitching moment with normal force for the wing with and without strake at Mach 0.8 and 1.2 are given in Fig. 14. The lift increment of the wing with strake at Mach 0.8 is obvious. It amounts to about 12-50% of the lift of the wing without strake at angles of attack of 10-20 deg. The moment curve at Mach 0.8 is quite similar to that at low speed. The nose-up trends at low and high angles of attack correspond to the formation and breakdown of the strake vortex, respectively. The lift curve slope of the wing with strake drops down

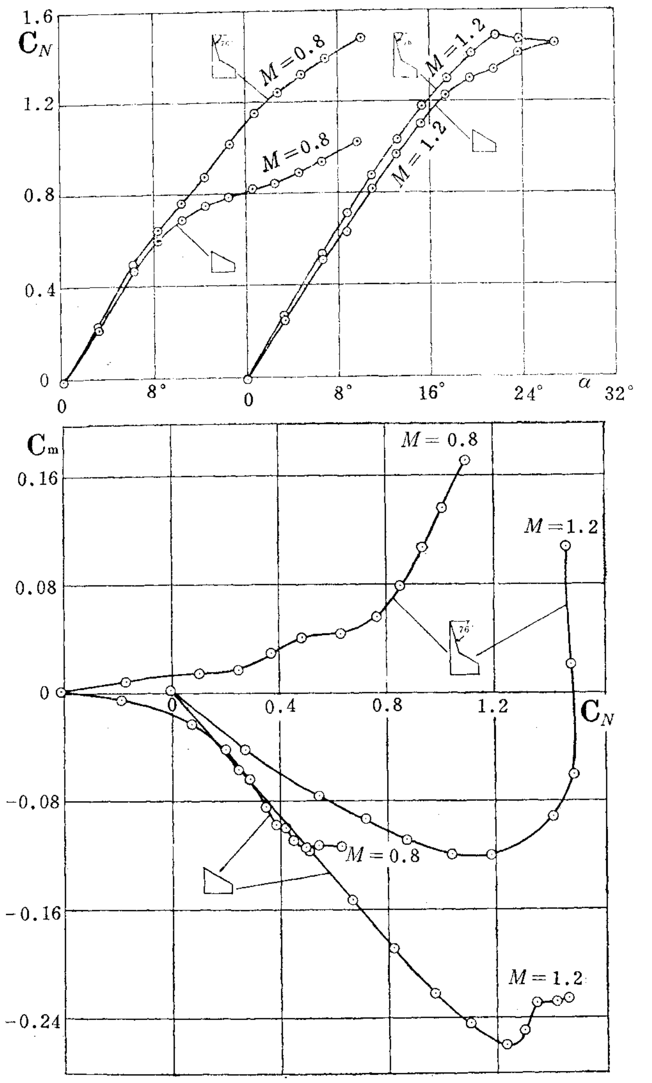

Fig. 14 Effect of Mach number on normal force and pitching moment.

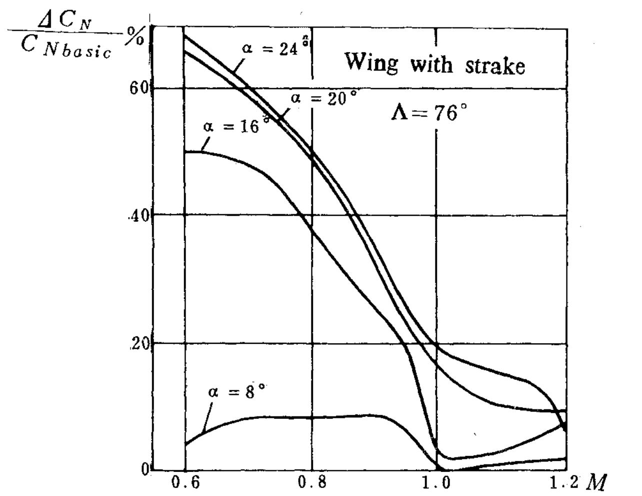

Fig. 15 Variations of normal force increment with transonic Mach number.

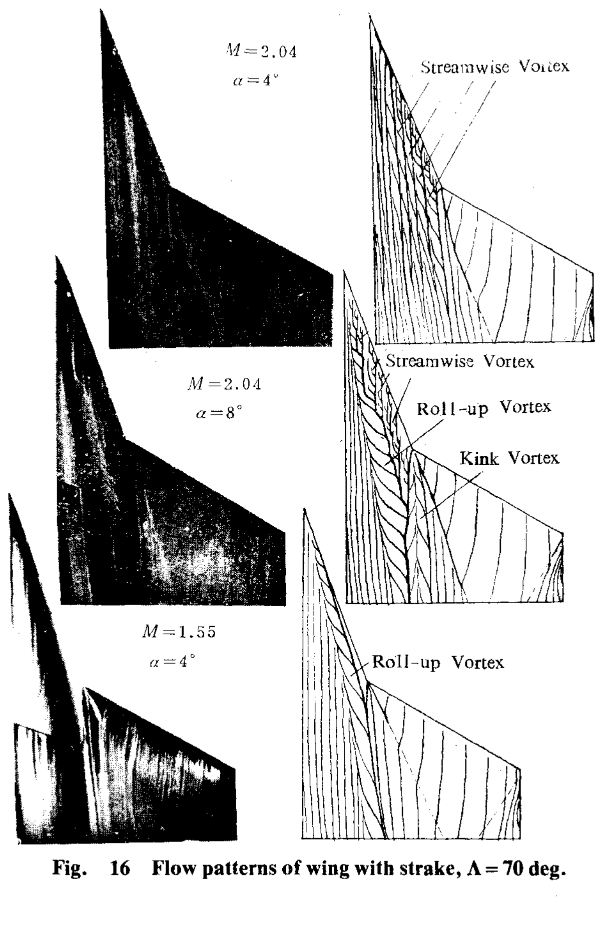

Fig. 16 Flow patterns of wing with strake, $\Lambda = 70$ deg.

suddenly and there is a sudden nose-up moment at Mach 1.2 at high angle of attack. This appears when the flow pattern of the outer panel is changed from leading edge attached flow with shock-induced separation to leading edge separation, while on the inner panel there is a breakdown of the strake vortex.

With increased Mach number at transonic speeds the lift increment of the wing with strake is decreased as shown in Fig. 15. This is primarily due to the fact that at higher Mach number the wing without strake maintains the leading edge attached flow to higher angle of attack and the wing stall is delayed. As Mach number is increased from 0.8 to 1.2, the moment curve is changed from subsonic to supersonic type, as shown in Fig. 14.

Supersonic Flow

Typical flow patterns of the wing with strake having leading edge sweepback of 70 deg at Mach 1.55 and 2.04 and at angles of attack of 4 and 8 deg are shown in Fig. 16. These figures show a leading edge attached flow, wing tip and kink vortices, and wing tip and kink shocks or shock-induced separation on the outer panel.

The flow patterns on the inner panel at supersonic speed depend upon the angle of attack, Mach number, and the strake leading edge sweepback. As the angle of attack is increased from 4 to 8 deg, the flow pattern changes from streamwise vortices to a coexistence of streamwise vortices and rolled-up vortex. As Mach number is increased from 1.55 to 2.04, the flow pattern changes from rolled-up vortex to streamwise vortices.

Although the flow patterns of wing with strake are complex at supersonic speed, the lift curve is linear. There is a nose-up moment at angles of attack higher than 4 deg, however, arising from the formation and development of the strake vortex.

The lift/drag ratio of the wing with strake is greater than that of the wing without strake at supersonic speeds throughout the range of lift coefficients, as shown in Fig. 9. This is due to a decrease in drag and not an increase in lift. The decrease in zero-lift drag comes from the decrease in

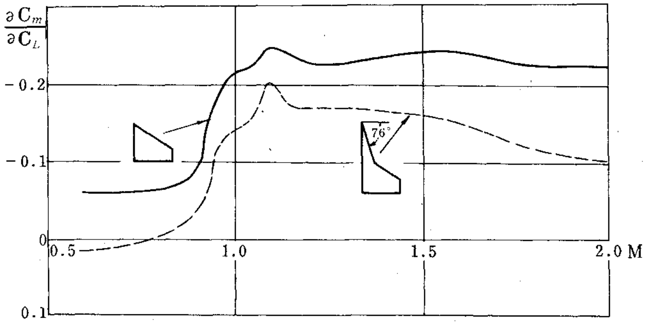

Fig. 17 Variation of $\partial C_m / \partial C_L$ with Mach number.

thickness chord ratio, while the decrease in trim drag is caused by less backward movement of the aerodynamic center, as shown in Fig. 17.

Conclusions

As a a result of present experimental investigation of a wing with strake, several conclusions can be drawn:

1) The flow on the whole upper wing surface is affected and controlled by the formation, development, and breakdown of the strake vortex. Four flow types at low speed can be distinguished: completely attached flow; coexistence of strake vortex and attached flow; coexistence of strake vortex and bubble vortex; and strake vortex breakdown.

2) The lift increase results from the effect of the strake vortex not only on the strake and aft inner panel but also on the outer panel.

3) Adding the strake to the wing at low speed results in a nonlinear pitching moment variation at low and high angles of attack. This is mainly due to the effect of the formation and breakdown of the strake vortex on the wing as well as on the horizontal tail. Methods described can effectively reduce the nonlinearity of the pitching moment.

4) The lift increment is decreased with an increase in Mach number at transonic speeds. This is primarily due to the fact that the flow pattern over the wing without strake changes from leading edge separation to leading edge attached flow with shock-induced separation.

5) At supersonic speeds the lift/drag ratio of the wing with strake is increased throughout the range of lift. This is due primarily to the decrease in drag rather than an increase in lift as at low speed.

References

[1] Staudacher, W., "Verbesserung der Manoever Leistungen im honen Unterschall," *DLR Mitteilung,* Vol. 73, No. 4, pp. 137-158.

[2] Staudacher, W., "Zum Einfluss von Flügelgrundriss-Modifikationen auf die Aerodynamischen Leistungen von Kampfflugzeugen," Deutsche Gesellschaft für Luft-und Raumfahrt 73-71, 1973, p. 9.

[3] Ray, E.J., Mckinney, L.W., and Carmichael, J.G., "Maneuver and Buffet Characteristics of Fighter Aircraft," NASA TN D-7131, 1973.

[4] Henderson, W.P. and Huffman, J.K., "Effect of Wing Design on the Longitudinal Aerodynamic Characteristics of a Wing-Body Model at Subsonic Speeds," NASA TN D-7099, 1972.

[5] Lamar, J.E., "Strake-Wing Analysis and Design," AIAA Paper 78-1201, also *Journal of Aircraft,* Vol. 17, Jan. 1980, pp. 20-27.

[6] Luckring, J.M., "Theoretical and Experimental Aerodynamics of Strake-Wing Interactions up to High Angles-of-Attack," AIAA Paper 78-1202, also *Journal of Aircraft,* Vol. 16, Nov. 1979, pp. 756-762.

[7] Küchemann, D., "Types of Flow on Swept Wings with Special Reference to Free Boundaries and Vortex Sheets," *Journal of Royal Aeronautical Society,* Vol. 57, Nov. 1953, pp. 683-699.

[8] Squire, L.C., Jones, G., and Stanbrook, A., "An Experimental Investigation of the Characteristics of Some Plane and Cambered 65° Delta Wings at Mach Numbers from 0.7 to 2.0," A.R.C. R.&M. 3305, 1963.

[9] Liu, M.J., Lü, Z.Y., and Gao, X.K., "Flow Patterns of a Strake-Wing at Low Speed," (in Chinese) Beijing Institute of Aeronautics and Astronautics (BIAA), China, BH-B265, Jan. 1976.

[10] Qiu, C.H., and Cheng, Y.X., "Force Tests of a Strake- Wing at Low-Speed," (in Chinese) BIAA, China, BH-B266, Jan. 1976.

[11] Su, W.H., and Lü, Z.Y., "Flow Patterns of a Strake- Wing at Supersonic Speeds," (in Chinese) BIAA, China, BH-B305, Oct. 1977.

[12] Liu, M.J., and Gao, X.K., "Force Tests of a strake-wing at supersonic speeds," (in Chinese) BIAA, China, BH-B306, Oct. 1977.